

**Novel redox active rhodium(III) complex with bis(arylimino)acenaphthene ligand: synthesis, structure and electrochemical studies**

**Artem L. Gushchin, Nikolai F. Romashev, Alexandra A. Shmakova, Pavel A. Abramov, Maxim R. Ryzhikov, Iakov S. Fomenko and Maxim N. Sokolov**

**Table of Contents**

**Experimental section**

**References**

**Figure S1.** <sup>1</sup>H NMR spectrum of **1** in DMSO-d<sub>6</sub> and peak assignments.

**Figure S2.** UV-vis spectrum of **1** in DMF.

**Figure S3.** Cyclic voltammogram of 1 mM solution of **1** in MeCN in the ranges from 0 to 2.0 V and from 0 to -2.0 V with a scan rate of 100 mV/s.

**Figure S4.** Cyclic voltammograms of 1 mM solution of **1** in MeCN recorded in Ar (black line), and in the presence of CO<sub>2</sub> (red line), scan rate 100 mV/s.

**Figure S5.** Molecular structure of **1** showing a positional disordering of H<sub>2</sub>O and Cl<sup>-</sup> in two terminal sites of Rh.

**Figure S6.** Crystal packing for **1**·CH<sub>2</sub>Cl<sub>2</sub>.

**Figure S7.** Optimized structure of **1** and [Rh<sup>I</sup>(dpp-bian)(H<sub>2</sub>O)Cl] complexes.

**Table S1.** Summary of crystal data for **1**·CH<sub>2</sub>Cl<sub>2</sub>.

**Table S2.** Selected geometric parameters (Å) for **1**·CH<sub>2</sub>Cl<sub>2</sub>.

**Table S3.** Selected interatomic distances (*d*, Å) calculated at BLYP+D3BJ/TZP for **1**<sup>n</sup> (n = 0, -1, +1) and [Rh<sup>I</sup>(dpp-bian)(H<sub>2</sub>O)Cl].

## EXPERIMENTAL SECTION

**General Procedures.** All the experiments were carried out in air. All commercially available reagents ( $\text{RhCl}_3 \cdot 3\text{H}_2\text{O}$ ) were used as purchased. 1,2-Bis[(2,6-diisopropylphenyl)imino]acenaphthene (dpp-bian) was prepared as reported [S1]. Organic solvents (MeOH,  $\text{CH}_2\text{Cl}_2$ , MeCN,  $\text{Et}_2\text{O}$  and hexane) were dried by standard methods before use.

**Physical Measurements.** Elemental C, H, N analyses were performed with a EuroEA3000 Eurovector analyzer. IR spectra were recorded in the  $4000\text{--}300\text{ cm}^{-1}$  range with a Perkin–Elmer System 2000 FTIR spectrometer with samples in KBr pellets.  $^1\text{H}$  NMR spectra were acquired on a Bruker Avance-500 spectrometer with a 5mm PABBO-PLUS probe. The chemical shifts were given in parts per million from  $\text{SiMe}_4$ . The cyclic voltammograms (CV) were recorded with a 797 VA Computrace system (Metrohm, Switzerland). All measurements were performed with a conventional three-electrode configuration consisting of glassy carbon working and platinum auxiliary electrodes and an  $\text{Ag}/\text{AgCl}/\text{KCl}$  reference electrode. The solvent used in all experiments was MeCN which was deoxygenated before use. Tetra-*n*-butylammonium hexafluorophosphate (0.1 M solution) was used as a supporting electrolyte. The concentration of the complex **1** was  $1 \cdot 10^{-3}$  M. Redox potential values ( $E_{1/2}$ ) were determined as  $(E_a + E_c)/2$ , where  $E_a$  and  $E_c$  are anodic and cathodic peak potentials, respectively. For experiments with carbon dioxide, the solution of **1** in  $\text{CH}_3\text{CN}$  was saturated with  $\text{CO}_2$  by bubbling for 20 min.

### Synthesis of $[\text{Rh}(\text{dpp-bian})(\text{H}_2\text{O})\text{Cl}_3] \cdot \text{CH}_2\text{Cl}_2$ (**1**· $\text{CH}_2\text{Cl}_2$ )

Salt  $\text{RhCl}_3 \cdot 3\text{H}_2\text{O}$  (70 mg, 0.308 mmol) and dpp-bian (154 mg, 0.308 mmol) were dissolved in MeOH (30 ml). The mixture was stirred at reflux for 12 hours. The resulting dark red solution was taken to dryness by rotary evaporation, and the solid residue was re-dissolved in dichloromethane (5 ml). The analytically pure product was obtained by adding a large excess of hexane to the solution in dichloromethane. Yield: 100 mg (40%). Crystals suitable for XRD were obtained by slow evaporation of the dichloromethane solution. Anal. Calc. for  $\text{C}_{37}\text{H}_{44}\text{N}_2\text{Cl}_5\text{ORh}$ : C, 54.6; H, 5.5; N, 3.5%. Found: C, 54.2; H, 5.6; N, 3.8%. IR (KBr,  $\nu$ ,  $\text{cm}^{-1}$ ): 3347(w), 3176(m), 3058(w), 2970(s), 2928(s), 2865(m), 1659(w), 1619(w), 1597(m), 1570(m), 1487(w), 1463(m), 1434(m), 1417(m), 1383(m), 1361(m), 1324(w), 1293(m), 1273(m), 1221(w), 1181(w), 1148(w), 1085(w), 1058(w), 1042(w), 961(w), 938(w), 834(s), 799(s), 781(s), 758(s), 728(s), 698(m), 647(w), 624(w), 546(m), 481(w), 408(w).  $^1\text{H}$  NMR (500 MHz, 298 K,  $\text{DMSO-d}_6$ ):  $\delta$  0.57-0.73 (m, 12H,  $\text{CH}_3$  (ipr)), 1.20-1.36 (m, 12H,  $\text{CH}_3$  (ipr)), 3.75-4.05 (m, 4H, CH (ipr)), 6.29-6.54 (m, 2H,  $\text{H}_3$ ), 7.35-7.75 (m, 8H,  $\text{H}_{4,10,11,12}$ ), 8.30-8.39 (m, 2H,  $\text{H}_5$ ) ppm. UV/vis (DMF,  $\lambda_{\text{max}}$ , nm ( $\epsilon$ )): 285 ( $2.8 \cdot 10^4$ ), 359 sh ( $7.0 \cdot 10^3$ ), 451 ( $3.8 \cdot 10^4$ ).

**Computational details.** Geometry optimization of complex **1** and its oxidized (**1**<sup>+</sup>) and reduced (**1**<sup>-</sup>) species as well as double reduced Rh(I) complex, [Rh(bian)(H<sub>2</sub>O)Cl], was performed in ADF2017 [S2,S3] program suit with BLYP [S4–S7] density functional, Grimme D3BJ [S8] dispersion correction and all-electron TZP [S9] basis set. Zero order regular approximation (ZORA) [S10] and Conductor like Screening Model (COSMO) [S11] were used to take into account scalar relativistic effects and acetonitrile environment, respectively. All geometries were optimized at C<sub>1</sub> symmetry and characterized by the absence of imaginary frequencies. Spin unrestricted method were used for **1**<sup>+</sup> and **1**<sup>-</sup> species. In order to analyze molecular orbitals, geometries optimized at BLYP+D3BJ/TZP level of theory were used for single point calculations with hybrid B3LYP [S12] density functional, Grimme D3BJ dispersion correction, all-electron TZP basis set, ZORA and COSMO.

### Single-crystal X-ray analysis

The diffraction data for **1**·CH<sub>2</sub>Cl<sub>2</sub> were collected on a Bruker Apex Duo diffractometer with MoK $\alpha$  radiation ( $\lambda = 0.71073$ ) by doing  $\varphi$  and  $\omega$  scans of narrow (0.5°) frames at 150 K. Absorption correction was done empirically using SADABS [S13]. Crystallographic data and refinement details for **1**·CH<sub>2</sub>Cl<sub>2</sub> are given in Table S1.

The structure was solved by direct method and refined by full-matrix least-squares treatment against  $|F|^2$  in anisotropic approximation with SHELX 2017/1 [S14] in ShelXle program [S15]. Hydrogen atoms were refined in geometrically calculated positions.

In the crystal structure of **1**·CH<sub>2</sub>Cl<sub>2</sub> there is a positional disordering of H<sub>2</sub>O and Cl<sup>-</sup> in two terminal sites of Rh. In the case of O1/Cl4 calculated occupancies are 0.8/0.2 which gives dividing of H<sub>2</sub>O and Cl<sup>-</sup> positions. In the case of O2/Cl3 calculated occupancies were found as 0.2/0.8 and positions of H<sub>2</sub>O and Cl<sup>-</sup> cannot be divided.

The crystallographic data have been deposited in the Cambridge Crystallographic Data Centre under the deposition code CCDC 1849307.

## References

- [S1] A. Paulovicova, U. El-Ayaan, K. Shibayama, T. Morita, Y. Fukuda, Mixed-Ligand Copper(II) Complexes with the Rigid Bidentate Bis(N-arylimino)acenaphthene Ligand: Synthesis, Spectroscopic-, and X-ray Structural Characterization, *Eur. J. Inorg. Chem.* 2001 (2001) 2641–2646. doi:10.1002/1099-0682(200109)2001:10<2641::AID-EJIC2641>3.0.CO;2-C.
- [S2] G. te Velde, F.M. Bickelhaupt, E.J. Baerends, C. Fonseca Guerra, S.J.A. van Gisbergen, J.G. Snijders, T. Ziegler, Chemistry with ADF, *J. Comput. Chem.* 22 (2001) 931–967. doi:10.1002/jcc.1056.
- [S3] ADF2016, SCM, Theoretical Chemistry, Vrije Universiteit, Amsterdam, The Netherlands, <http://www.scm.com>, (2016).
- [S4] A.D. Becke, Density-functional exchange-energy approximation with correct asymptotic behavior, *Phys. Rev. A.* 38 (1988) 3098–3100. doi:10.1103/PhysRevA.38.3098.
- [S5] C. Lee, W. Yang, R.G. Parr, Development of the Colle-Salvetti correlation-energy formula into a functional of the electron density, *Phys. Rev. B.* 37 (1988) 785–789. doi:10.1103/PhysRevB.37.785.
- [S6] B.G. Johnson, P.M.W. Gill, J.A. Pople, The performance of a family of density functional methods, *J. Chem. Phys.* 98 (1993) 5612–5626. doi:10.1063/1.464906.
- [S7] T. V. Russo, R.L. Martin, P.J. Hay, Density functional calculations on first-row transition metals, *J. Chem. Phys.* 101 (1994) 7729–7737. doi:10.1063/1.468265.
- [S8] S. Grimme, S. Ehrlich, L. Goerigk, Effect of the damping function in dispersion corrected density functional theory, *J. Comput. Chem.* 32 (2011) 1456–1465. doi:10.1002/jcc.21759.
- [S9] E. Van Lenthe, E.J. Baerends, Optimized Slater-type basis sets for the elements 1-118, *J. Comput. Chem.* 24 (2003) 1142–1156. doi:10.1002/jcc.10255.
- [S10] E. van Lenthe, A. Ehlers, E.-J. Baerends, Geometry optimizations in the zero order regular approximation for relativistic effects, *J. Chem. Phys.* 110 (1999) 8943–8953. doi:10.1063/1.478813.
- [S11] C.C. Pye, T. Ziegler, An implementation of the conductor-like screening model of solvation within the Amsterdam density functional package, *Theor. Chem. Accounts Theory, Comput. Model. (Theoretica Chim. Acta)*. 101 (1999) 396–408. doi:10.1007/s002140050457.
- [S12] P.J. Stephens, F.J. Devlin, C.F. Chabalowski, M.J. Frisch, Ab Initio Calculation of Vibrational Absorption and Circular Dichroism Spectra Using Density Functional Force Fields, *J. Phys. Chem.* 98 (1994) 11623–11627. doi:10.1021/j100096a001.
- [S13] SHELDRICK, G. M., Program for Empirical Absorption Correction of Area Detector Data, SADABS. (1996). <https://ci.nii.ac.jp/naid/10011313791/> (accessed June 16, 2019).
- [S14] G.M. Sheldrick, IUCr, *SHELXT* – Integrated space-group and crystal-structure determination, *Acta Crystallogr. Sect. A Found. Adv.* 71 (2015) 3–8. doi:10.1107/S2053273314026370.
- [S15] C.B. Hübschle, G.M. Sheldrick, B. Dittrich, IUCr, *ShelXle* : a Qt graphical user interface for *SHELXL*, *J. Appl. Crystallogr.* 44 (2011) 1281–1284. doi:10.1107/S0021889811043202.

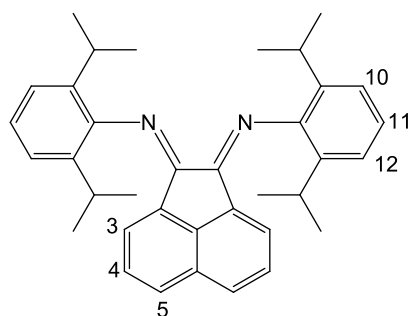
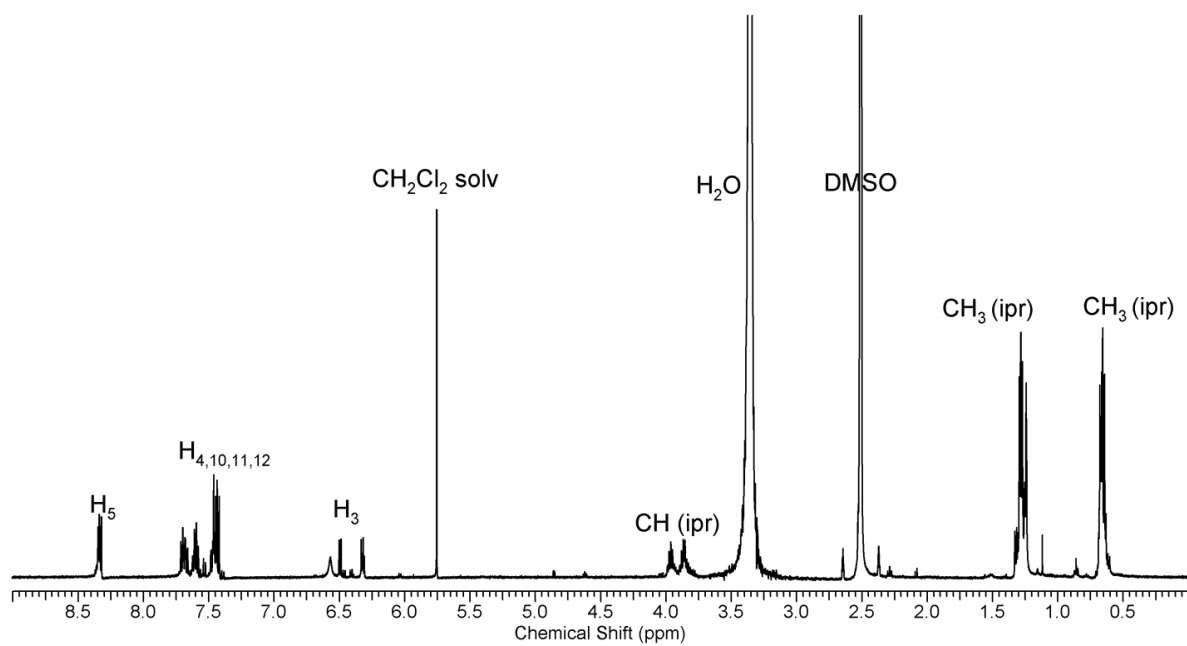


**Figure S1.**  $^1\text{H}$  NMR spectrum of **1** in  $\text{DMSO-d}_6$  and peak assignments

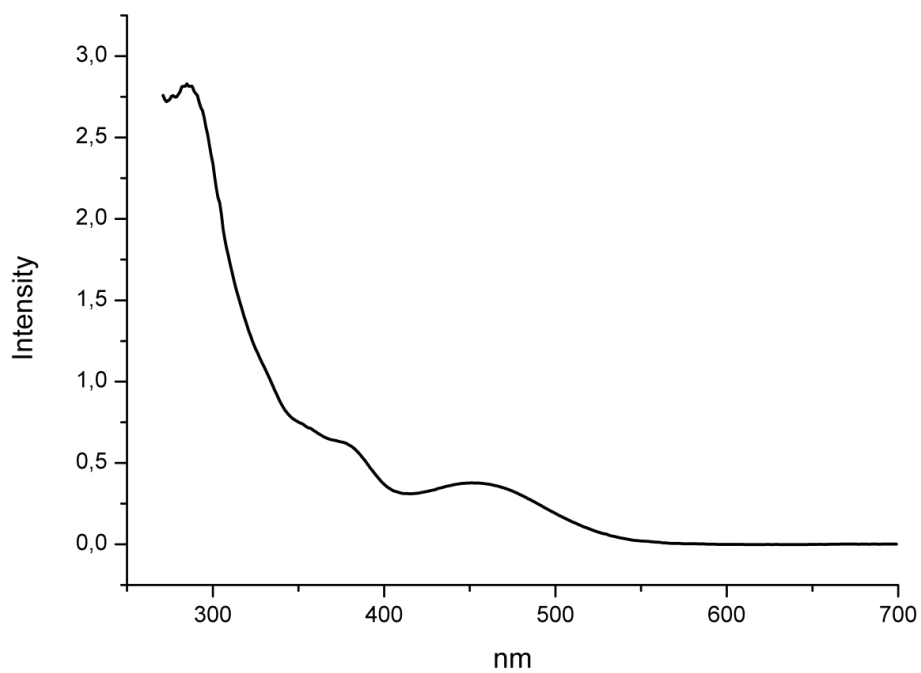


**Figure S2.** UV-vis spectrum of **1** in DMF

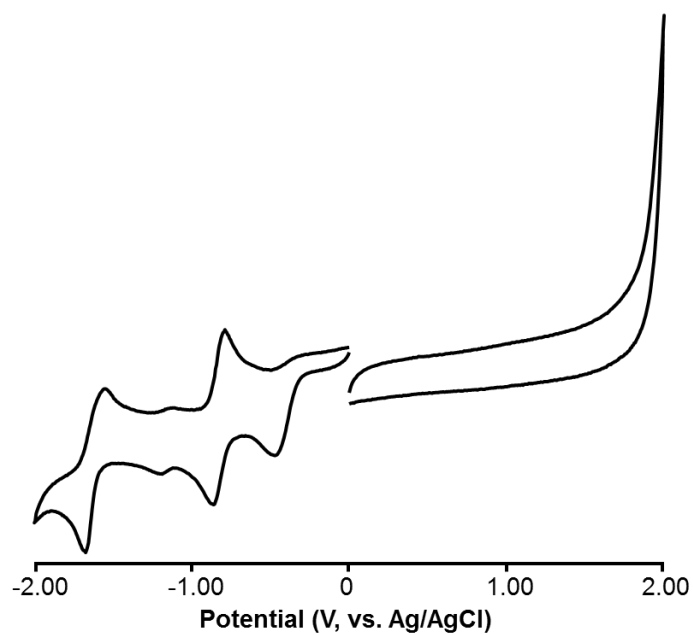


**Figure S3.** Cyclic voltammogram of 1 mM solution of **1** in CH<sub>3</sub>CN in the ranges from 0 to 2.0 V and from 0 to -2.0 V with a scan rate of 100 mV/s

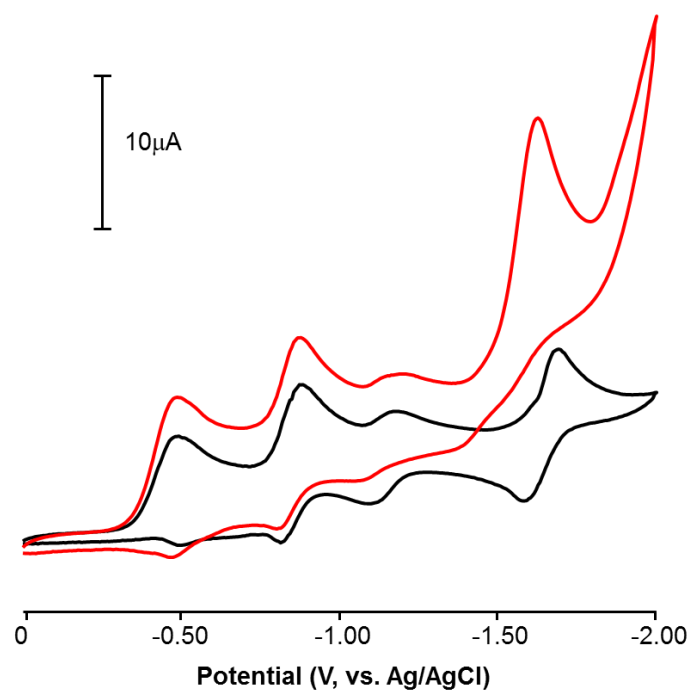


**Figure S4.** Cyclic voltammograms of 1 mM solution of **1** in CH<sub>3</sub>CN recorded in Ar (black line), and in the presence of CO<sub>2</sub> (red line), scan rate 100 mV/s. No peaks were found in the cyclic voltammogram of a saturated solution of CO<sub>2</sub> in CH<sub>3</sub>CN without **1** in the range from 0 to -2 V

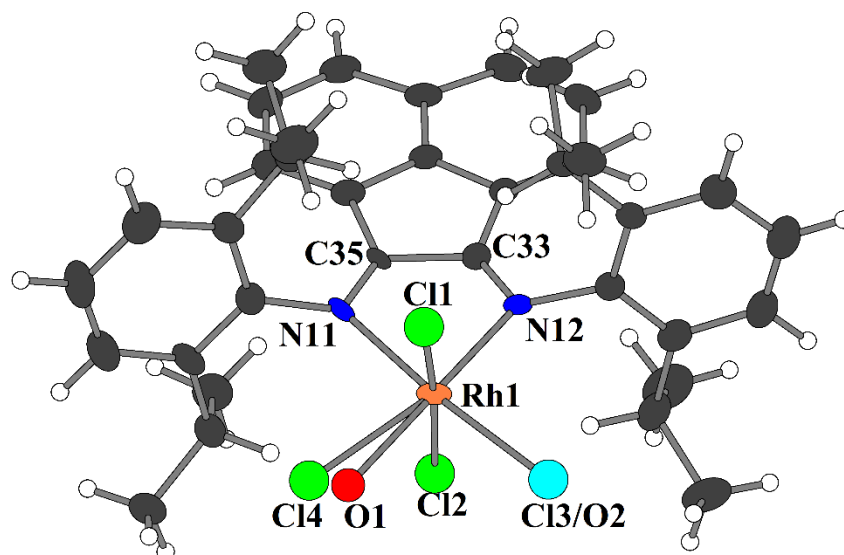


**Figure S5.** Molecular structure of **1** showing a positional disordering of H<sub>2</sub>O and Cl<sup>-</sup> in two terminal sites of Rh.

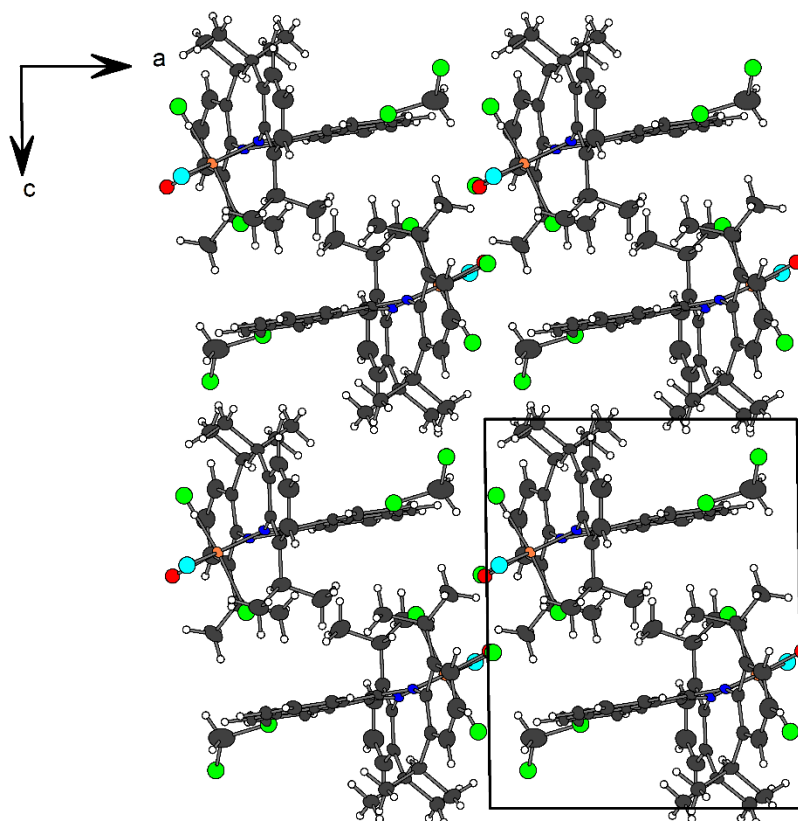


**Figure S6.** Crystal packing for **1**·CH<sub>2</sub>Cl<sub>2</sub>

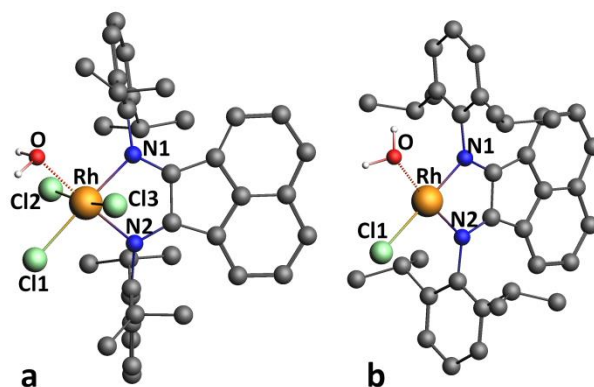


**Figure S7.** Optimized structure of  $1^0$  and  $[\text{Rh}^{\text{I}}(\text{dpp-bian})(\text{H}_2\text{O})\text{Cl}]$  complexes

**Table S1.** Summary of crystal data for  $1 \cdot \text{CH}_2\text{Cl}_2$ .

	$1 \cdot \text{CH}_2\text{Cl}_2$
Empirical formula	$\text{C}_{37}\text{H}_{44}\text{Cl}_5\text{N}_2\text{ORh}$
$M_r$	812.90
Crystal system, space group	Triclinic, $P\bar{1}$
Temperature (K)	150
$a, b, c$ (Å)	11.191 (4), 12.066 (4), 14.055 (5)
$\alpha, \beta, \gamma$ (°)	76.987 (11), 86.812 (10), 79.358 (11)
$V$ (Å <sup>3</sup> )	1817.2 (11)
$Z$	2
Radiation type	Mo $K\alpha$
$\mu$ (mm <sup>-1</sup> )	0.87
Crystal size (mm)	0.33 × 0.29 × 0.23
Diffractometer	Bruker Apex Duo
Absorption correction	Multi-scan SADABS (Bruker-AXS, 2004)
$T_{\text{min}}, T_{\text{max}}$	0.670, 0.747
No. of measured, independent and observed [ $I > 2\sigma(I)$ ] reflections	14696, 7277, 5146
$R_{\text{int}}$	0.037
$\theta$ values (°)	$\theta_{\text{max}} = 27.1, \theta_{\text{min}} = 1.8$
$(\sin \theta/\lambda)_{\text{max}}$ (Å <sup>-1</sup> )	0.642
Range of $h, k, l$	$-14 \leq h \leq 13, -15 \leq k \leq 15, -17 \leq l \leq 17$
$R[F^2 > 2\sigma(F^2)], wR(F^2), S$	0.057, 0.200, 0.98
No. of reflections, parameters, restraints	7277, 409, 0
H-atom treatment	H-atom parameters constrained
Weighting scheme	$w = 1/[\sigma^2(F_o^2) + (0.1424P)^2]$ where $P = (F_o^2 + 2F_c^2)/3$
$\Delta\rho_{\text{max}}, \Delta\rho_{\text{min}}$ (e Å <sup>-3</sup> )	2.17, -1.76

**Table S2.** Selected geometric parameters (Å) for **1**·CH<sub>2</sub>Cl<sub>2</sub>.

Rh1—O1	2.048 (5)	Cl2—Rh1	2.3423 (13)
N11—Rh1	2.067 (4)	Cl3/O2—Rh1	2.3362 (16)
N12—Rh1	2.033 (4)	Cl4—Rh1	2.452 (10)
Cl1—Rh1	2.3176 (13)	C33—N12	1.307(6)
C33—C35	1.487(7)	C35—N11	1.293(6)

**Table S3.** Selected interatomic distances (*d*, Å) calculated at BLYP+D3BJ/TZP for **1**<sup>n</sup> (n = 0, -1, +1) and [Rh<sup>I</sup>(dpp-bian)(H<sub>2</sub>O)Cl].

	<b>1</b> <sup>0</sup>	<b>1</b> <sup>-</sup>	<b>1</b> <sup>+</sup>	[Rh <sup>I</sup> (dpp-bian)(H <sub>2</sub> O)Cl]
Rh-N1	2.10	2.10	2.13	2.01
Rh-N2	2.05	2.06	2.06	2.0
Rh-Cl1	2.41	2.46	2.37	2.40
Rh-Cl2	2.40	2.41	2.37	-
Rh-Cl3	2.41	2.43	2.37	-
Rh-O	2.17	2.21	2.17	2.18